Mechanochromic luminescence and liquid crystallinity of molecular copper clusters

Brendan Huitorel, Quentin Benito, Alexandre Fargues, Alain Garcia, Thierry Gacoin, Jean-Pierre Boilot, Sandrine Perruchas, Franck Camerel

Mechanochromic Luminescence and Liquid Crystallinity of Molecular Copper Clusters

Brendan Huitorel,[a] Quentin Benito,[a] Alexandre Fargues,[b] Alain Garcia,[b] Thierry Gacoin,[a] Jean-Pierre Boilot,[a] Sandrine Perruchas,[a] and Franck Camerel[c]**

[a] Laboratoire de Physique de la Matière Condensée (PMC), Ecole Polytechnique - CNRS, 91128 Palaiseau Cedex, France.
E-mail: sandrine.perruchas@polytechnique.edu

[b] Institut de Chimie de la Matière Condensée de Bordeaux (ICMCB) - CNRS, 87 Avenue du Docteur A. Schweitzer, 33608 Pessac Cedex, France.

[c] Laboratoire Matière Condensée et Systèmes Électroactifs (MaCSE), Institut des Sciences Chimiques de Rennes, UMR 6226 CNRS-Université de Rennes 1, Campus de Beaulieu, 35042 Rennes, France. Email: franck.camerel@univ-rennes1.fr

Abstract. Molecular copper iodide clusters with the $[Cu_4I_4]$ cubane core have been functionalized by phosphine ligands carrying protomesogenic gallate-based derivatives bearing either long alkyl chains (C8, C12 and C16) or cyanobiphenyl (CBP) fragments. The mesomorphic properties of the functionalized clusters were studied by combining differential scanning calorimetry (DSC), polarized optical microscopy (POM) and small angle X-ray scattering (SAXS) experiments. Whereas clusters functionalized solely with long alkyl chains present amorphous or crystalline states, the cluster carrying CBP fragments displays liquid crystal properties with the formation of a smectic A mesophase from room temperature up to 100 °C. Temperature-dependent photoluminescence measurements show that the CBP derivative displays an unusual luminescence thermochromism which is possibly due to a resonance energy transfer mechanism between the emissive $[Cu_4I_4]$ inorganic and CBP moieties. The emission properties of this original cluster are also sensitive to variation of local order of the molecular assembly. Moreover, the liquid crystalline properties imported on the inorganic core allow for a facile deformation of its local environment leading to mechanochromic properties related to modulation of intramolecular interactions. Indeed, mechanical constraints on the molecularly self-assembled structure induce changes at the molecular level by modification of the $[Cu_4I_4]$ inorganic cluster core geometry and in particular of the strength of the cuprophilic interactions.

Introduction.

In the last ten years, stimuli-responsive luminescent materials have emerged as a new class of smart functional materials having potential applications in recording and sensor devices.[1,2,3] Materials displaying luminescence mechanochromism for which external mechanical force (grinding or shearing) is converted into visible light emission change, present great interest in the development of security systems, pressure mapping sensors[4] and memory devices for examples.[5,6,7,8,9,10,11,12]

The mechanochromic luminescent materials are in great majority based on organic dyes[13] and in less extent on transition metal complexes.[14] Because the solid-state luminescence properties of molecular materials depend on the molecular structure and structural arrangements of the molecules, the mechanochromism mechanism is usually depicted as modifications of the inter-molecular interactions upon mechanical solicitations, leading to changes of the packing mode and eventually of the emitting energy states. Reversibility of the phenomenon is usually achieved by restoring the structural arrangement (recrystallization) by thermal treatment or solvent exposure.[15]

For the development of mechanochromic materials, the study of liquid crystals appear as a relevant strategy.[16] These functional soft materials exhibit mobile and ordered states which can be easily deformed upon the application of an external stimulus thus inducing modifications of the molecularly assembled structures. The number of liquid crystal compounds exhibiting luminescence mechanochromic properties is still limited with mainly purely organic examples based on conjugated polyaromatic moieties.[17,18,19] The mechanochromism mechanism of these compounds is based on modifications of intermolecular interactions. Despite the rich photoluminescence properties of transition metal complexes,[20] only few compounds based on platinum,[21,22] and iridium[23] metals have been reported so far.

The molecular copper(I) iodide clusters constitute a relevant family of photoactive compounds by exhibiting remarkable optical properties.[24,25] In particular, $[Cu_4I_4L_4]$ (L = organic ligand) cubane clusters exhibits luminescence properties highly sensitive to their solid-state organization *via* intermolecular interactions,[26] leading to stimuli-responsive properties. These compounds are indeed rare examples combining both luminescence mechanochromism and thermochromism: a particularly appealing property for developing multifunctional sensing systems.[27,28,29,30] However, the rational synthesis of such compounds is still a great challenge. In this context, combining the sensitive photoluminescence properties of copper iodide clusters with the flexible self-assembly properties of liquid crystals is thus very promising to develop original stimuli-responsive photoactive materials.

Here, we report on the study of metallomesogens based on $[Cu_4I_4L_4]$ copper iodide clusters. In order to obtain such clusters exhibiting mesomorphic properties, two strategies have been explored. The first one is the grafting of long lypophilic alkyl chains onto the $[Cu_4I_4]$ cubane core and the second one is the direct grafting of mesomorphic promoters through flexible spacers. The latter is known to induce mesomorphic properties to unconventional core with isotropic geometry such as fullerene,[31] metal complexes[32] or metallic clusters.[33] Both strategies aim at improving interfaces and areas compatibilities between the rigid inorganic cores and the soft organic moieties and to enhance micro-segregation processes leading to liquid crystalline properties. Therefore, the $[Cu_4I_4]$ cubane cluster core has been functionalized by phosphine ligands carrying protomesogenic gallate-based derivatives bearing either long alkyl chains (C8, C12 and C16) or cyanobiphenyl (CBP) fragments (Figure 1). The mesomorphic properties of the functionalized clusters namely **CUB-Cn (n = 8, 12, 16)** or **CUB-CBP**, were studied by combining differential scanning calorimetry (DSC), polarized optical microscopy (POM) and small angle X-ray scattering (SAXS) experiments. Whereas clusters functionalized solely with long alkyl chains present amorphous or crystalline states, **CUB-CBP** cluster displays liquid crystal properties with the formation of a smectic A mesophase. Photophysical characterisations revealed luminescence thermochromism of the compounds and in particular of **CUB-CBP** with an unclassical behaviour. Indeed, due to the intrinsic luminescence properties of the CBP moiety,

CUB-CBP constitutes a dual emissive system presenting intriguing emission properties. Study of the evolution of **CUB-CBP** emission in function of its molecular organization has been conducted. Moreover, associated with its liquid crystal properties, the CBP derivative also displays luminescence mechanochromic properties with reversible modification of the emission wavelength in response to grinding. The correlation between the optical properties and the molecular organizations has been analyzed. Changes in the molecularly self-assembled structure induce a change at the molecular level by modification of the inorganic cluster core geometry and in particular of the strength of the intramolecular cuprophilic interactions.

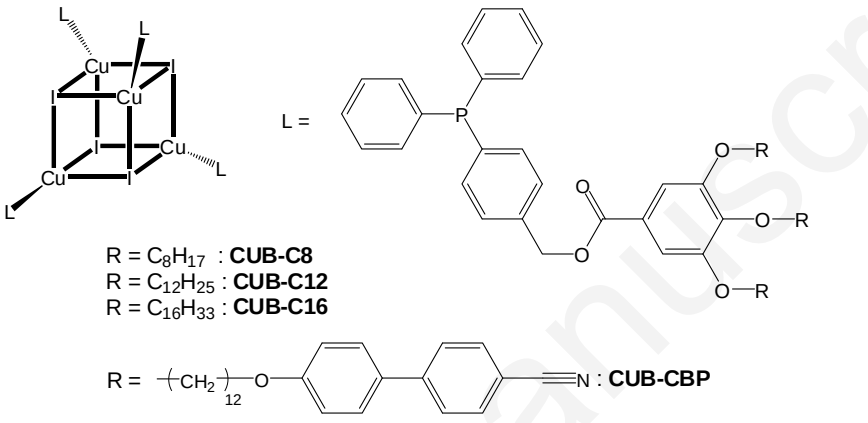

Figure 1. General representation of the functionalized $[Cu_4I_4L_4]$ copper iodide clusters (**CUB**) with the corresponding L ligands with **Cn** (n = 8, 12 and 16) for alkyl chains and **CBP** for cyanobiphenyl group.

Experimental Section.

Synthesis. All manipulations were performed with standard air-free techniques using schlenk equipment, unless otherwise noted. Solvents were distilled from appropriate drying agents and degassed prior to use. All the reactants were purchased from Aldrich or Fluka and used as received. 4-((diphenylphosphino)phenyl)methanol,[34] gallate derivatives carrying Cn (n = 8, 12, and 16) alkyl chains[35] or gallate derivative carrying CBP fragments[36] have been prepared as previously reported.

L-C8. A solution of 4-(diphenylphosphino)phenyl)methanol (200 mg, 0.68 mmol) in dichloromethane (5 mL) is added dropwise to a solution of DCC (169 mg, 0.82 mmol), DMAP (83.5 mg, 0.68 mmol) and of 3,4,5-trioctyloxybenzoic acid (347 mg, 0.74 mmol) in degassed dichloromethane (20 mL). The solution is stirred at room temperature overnight. After filtration and solvent evaporation, the product is purified by chromatography on silica gel (eluent: CH_2Cl_2 / petroleum ether, 1 / 1). After solvent evaporation and drying under vacuum, the ligand is obtained as colorless oil (379 mg, 0.49 mmol, Yield = 71 %). ^{1}H NMR (300 MHz, $CDCl_3$) δ (ppm): 0.89 (m, 9H, CH_3), 1.29 (m, 24H, CH_2), 1.47 (m, 6H, CH_2), 1.81 (m, 6H, CH_2), 4.00 (m, 6H, O-CH_2), 5.35 (s, 2H, CH_2), 7.17-7.70 (m, 16H, Ph). ^{31}P NMR (121 MHz, $CDCl_3$) δ (ppm) : -5.9. MS (ESI-TOF): m/z calcd [M+], 781.05; found, 781.41. **L-C12.** A solution of 4-(diphenylphosphino)phenyl)methanol (200 mg, 0.68 mmol) in dichloromethane (5 mL) is added dropwise to a solution of DCC (169 mg, 0.82 mmol), DMAP (83.5 mg, 0.68 mmol) and of 3,4,5- tridodecyloxybenzoic acid (462 mg, 0,68 mmol) in degassed dichloromethane (20 mL). The solution is stirred at room temperature overnight. After filtration and solvent evaporation, the product is purified by chromatography on silica gel (eluent: CH_2Cl_2 / petroleum ether, 1 / 1). After solvent evaporation and drying under vacuum, the ligand is obtained as colorless oil (484 mg, 0.51 mmol, Yield = 75 %). ^{1}H NMR (300 MHz, $CDCl_3$) δ (ppm): 0.89 (m, 9H, CH_3), 1.27 (m, 48H, CH_2), 1.47 (m, 6H, CH_2), 1.79 (m, 6H, CH_2), 4.01 (m, 6H, O-CH_2), 5.35 (s, 2H, CH_2), 7.29-7.41 (m, 16H, Ph). ^{31}P NMR (121 MHz, $CDCl_3$) δ (ppm) : -5.8. MS (ESI-TOF): m/z calcd [M+], 949.37; found, 949.97. **L-C16.** A solution of 4-(diphenylphosphino)phenyl)methanol (200 mg, 0.68 mmol) in dichloromethane (5 mL) is added dropwise to a solution of DCC (169 mg, 0.82 mmol), DMAP (83.5 mg, 0.68 mmol) and 3,4,5- trihexadecyloxybenzoic acid (577 mg, 0,68 mmol) in degassed dichloromethane (20 mL). The solution is stirred at room temperature overnight. After filtration and solvent evaporation, the product is purified by chromatography on silica gel (eluent: CH_2Cl_2 / petroleum ether, 1 / 2). After solvent evaporation, drying under vacuum and precipitation in a CH_2Cl_2/methanol mixture, the ligand is obtained as white powder (532 mg, 0.51 mmol, Yield = 75 %). ^{1}H NMR (300 MHz, $CDCl_3$) δ (ppm): 0.88 (m, 9H, CH_3), 1.25 (m, 72H, CH_2), 1.46 (m, 6H, CH_2), 1.79 (m, 6H, CH_2), 3.99 (m, 6H, O-CH_2), 5.30 (s, 2H, CH_2), 7.16-7.70 (m, 16H, Ph). ^{31}P NMR (121 MHz, $CDCl_3$) δ (ppm) : -5.9. MS (ESI-TOF): m/z calcd [M], 1117.69; found, 1118.02. Melting point = 54 °C. **L-CBP.** A solution of 4-(diphenylphosphino)phenyl)methanol (65 mg, 0.22 mmol) in dichloromethane (5 mL) is added dropwise to a solution of DCC (53 mg, 0.26 mmol), DMAP (22.4 mg, 0.18 mmol) and of the corresponding benzoic acid (230 mg, 0.18 mmol) in degassed dichloromethane (30 mL). The mixture is stirred at room temperature overnight. After solvent evaporation, the crude product is purified by silica gel chromatography (ethyl acetate/CH_2Cl_2, 1/20). After precipitation from a CH_2Cl_2/CH_3CN mixture, the ligand is obtained as a white solid (166 mg, 0.11 mmol, Yield = 60 %). ^{1}H NMR (300 MHz $CDCl_3$) δ (ppm) : 1.30 (m, 36H, CH_2), 1.47 (m, 12H, CH_2), 1.77 (m, 12H, CH_2), 3.99 (m, 12H, CH_2), 5.34 (s, 2H, CH_2), 6.97 (d, 6H, Ph), 7.28 (s, 2H, CH), 7.34-7.57 (m, 20H, Ph), 7.65 (m, 12H, Ph). ^{31}P NMR (121 MHz, $CDCl_3$) δ (ppm): -3.3. Anal. Calcd. (% wt.) for $C_{101}H_{114}PN_3O_8$, CH_3CN: C, 78.80; H, 7.51; N, 3.57; Found: C, 78.45; H, 7.83; N, 3.25. Melting point = 60 °C

CUB-C8. To a CuI (54 mg, 0.28 mmol) suspension in dichloromethane (20 mL) is added L-C8 ligand (200 mg, 0.26 mmol). The solution is stirred for 12 h at room temperature. After filtration and solvent evaporation, le product is purified by silica gel chromatography (eluent: CH_2Cl_2 / pentane, 4 / 1). After solvent evaporation and drying under vacuum, the product is obtained as a waxy material (118 mg, 0.030 mmol, Yield = 47 %). ^{1}H NMR (300 MHz, CD_2Cl_2) δ (ppm) : 0.87 (m, 9H, CH_3), 1.29 (m, 24H, CH_2), 1.45 (m, 6H, CH_2), 1.76 (m, 6H, CH_2), 3.97 (q, 6H, O-CH_2), 5.35 (s, 2H, CH_2), 7.30-7.38 (m, 10H, Ph), 7.51-7.57 (m, 6H, Ph). ^{31}P NMR (121 MHz, CD_2Cl_2) δ (ppm) : -22.5 (br). Anal. Calcd. (% wt.) for $C_{50}H_{69}PO_5CuI$: C, 61.82; H, 7.16; Found: C, 62.22; H, 7.25. **CUB-C12.** To a CuI (60 mg, 0.32 mmol) suspension in dichloromethane (20 mL) is added L-C12 ligand

(300 mg, 0.32 mmol). The solution is stirred for 12 h at room temperature. After filtration and solvent evaporation, le product is purified by silica gel chromatography (eluent: CH_2Cl_2 / cyclohexane, 2 / 1). After solvent evaporation and drying under vacuum, the cluster is obtained as a waxy material (244 mg, 0.054 mmol, Yield = 68 %). ^1H NMR (300 MHz, $CDCl_3$) δ (ppm) : 0.86 (m, 9H, CH_3), 1.25 (m, 48H, CH_2), 1.45 (m, 6H, CH_2), 1.74 (m, 6H, CH_2), 3.95 (q, 6H, O-CH_2), 5.33 (s, 2H, CH_2), 7.30-7.37 (m, 10H, Ph), 7.50-7.55 (m, 6H, Ph). ^1P NMR (121 MHz, $CDCl_3$) δ (ppm) : -20.3 (br). Anal. Calcd (% wt.) for $C_{62}H_{93}PO_5CuI$: C, 65.33; H, 8.22; Found: C, 65.76; H, 8.44. **CUB-C16.** To a CuI (50 mg, 0.26 mmol) suspension in dichloromethane (20 mL) is added L-C16 ligand (250 mg, 0.24 mmol). The solution is stirred for 12 h at room temperature. After filtration and solvent evaporation, le product is purified by silica gel chromatography (eluent: CH_2Cl_2 / cyclohexane, 2 / 1). After solvent evaporation and drying under vacuum, the product is obtained as a white solid (136 mg, 0.028 mmol, Yield = 46 %). ^1H NMR (300 MHz CD_2Cl_2) δ (ppm) : 0.86 (m, 9H, CH_3), 1.24 (m, 72H, CH_2), 1.41 (m, 6H, CH_2), 1.71 (m, 6H, CH_2), 3.95 (q, 6H, O-CH_2), 5.33 (s, 2H, CH_2), 7.29-7.37 (m, 10H, Ph), 7.50-7.56 (m, 6H, Ph). ^{31}P NMR (121 MHz, CD_2Cl_2) δ (ppm) : -19.0 (br). Anal. Calcd (% wt.) for $C_{74}H_{117}PO_5CuI$ + 4 CH_2Cl_2: C, 64.66; H, 8.61; Found: C, 64.64; H, 9.11. **CUB-CBP.** To a suspension of CuI (14 mg, 0.07 mmol) in dichloromethane (20 mL) was added L-CBP ligand (106 mg, 0.07 mmol). The solution was stirred for 12 h at room temperature. After filtration and evaporation, the white powder was purified by silica gel chromatography (eluent: CH_2Cl_2 / ethyl acetate, 20 / 1). After solvent evaporation, product is obtained as a white solid (104 mg, 0.015 mmol, Yield = 87 %). ^1H NMR (300 MHz CD_2Cl_2) δ (ppm) : 1.30 (m, 36 H, CH_2), 1.45 (m, 12 H, CH_2), 1.77 (m, 12 H, CH_2), 3.97 (m, 12 H, CH_2), 5.34 (s, 2 H, CH_2), 6.95 (d, 6 H, Ph), 7.24-7.37 (m, 10 H, Ph), 7.51-7.56 (m, 12 H, Ph), 7.65 (m, 12 H, Ph). ^{31}P NMR (121 MHz, CD_2Cl_2) δ (ppm): -22.7. Anal. Calcd (% wt.) for $C_{101}H_{114}PN_3O_8CuI$: C, 70.55; H, 6.68; N, 2.44; Found: C, 71.88; H, 7.15; N, 2.55.

Characterizations. ^1H and ^{31}P liquid NMR spectra were recorded on a Bruker Avance II spectrometer at room temperature, operating at the radiofrequency (rf) of 300 MHz. ^1H spectra were internally referenced from peaks of residual protons in deuterated solvents or from tetramethylsilane (TMS). A solution of H_3PO_4 85 % weight was used as an external standard for ^{31}P spectra. Elemental analyses (C, H, N) were performed by the Service de microanalyses de l'ICSN - CNRS Gif-sur-Yvette. Luminescence spectra were recorded on a SPEX Fluorolog FL 212 and on a Fluoromax-4 spectrofluorimeters (Horiba Jobin Yvon). The excitation source is a 450 Watt xenon lamp, excitation spectra were corrected for the variation of the incident lamp flux, as well as emission spectra for the transmission of the monochromator and the response of the photomultiplier. Low temperature measurements were recorded with a liquid helium circulation cryostat SMC TBT Air Liquid model C102084. The absolute internal quantum yields (Φ) were measured by using a Fluoromax-4 (Horiba Jobin Yvon) integrating sphere. UV-visible absorption spectra were recorded with a Varian Cary 50 spectrophotometer with dichloromethane solutions of the clusters and ligands. Differential scanning calorimetry (DSC) was carried out by using NETZSCH DSC 200 F3 instrument equipped with an intracooler. DSC traces were measured at 10 °C/min down to -25 °C. Optical microscopy investigations were performed on a Nikon H600L polarizing microscope equipped with a Linkam "liquid crystal pro system" hotstage. The microscope is also equipped with a UV irradiation source (Hg Lamp, λ = 340-380 nm) and an ocean optic USB 2000+ UV-Vis-NIR spectrophotometer based on CCD detection technology. X-ray scattering experiments (SAXS) were performed using a FR591 Bruker AXS rotating anode X-ray generator operated at 40 kV and 40 mA with monochromatic Cu Kα radiation (λ = 1.541 Å) and point collimation. The patterns were collected with a Mar345 Image-Plate detector (Marresearch, Norderstedt, Germany). Complementary SAXS measurements at lower angles (Figure 11) where performed at the LPS (Orsay, France) on a Rigaku rotating anode X-Ray generator operated at 40 kV and 40 mA using Cu radiation and equipped with a Pilatus detector. The samples were held in Lindeman glass capillaries (1 mm diameter). The molecular mechanics studies have been performed on the French supercomputer Occigen using the program suite Materials Studio (Forcite). A periodic cell containing 48 **CUB-CBP** molecular clusters was built according to the dimension given by the X-ray measurements and the molecular volume of the molecule (58.7x3/13x4/13x4 Å) (density = 1.07). After energy relaxation, the simulation consisted of a 1 ns isotherm at 333 K with the "universal" forcefield (NVT ensemble and 1 fs time step) in periodic boundary conditions.

Results and Discussion.

Synthesis and characterization of the metallomesogens.

Mesomorphic properties were introduced to the copper iodide clusters *via* the ligands. Previous study on copper iodide gelators showed the effective transfer of the self-assembled properties of the cholesteryl moieties of the ligands to the clusters.[37] Phosphine ligands bearing long alkyl chains and CBP (cyanobiphenyl) groups have been synthesized starting from 4-(diphenylphosphino)phenylmethanol (see experimental part and schemes S1-2). The ligands incorporating gallate derivatives possess alkyl chains of different length (C8, C12 and C16) or CBP moieties. CBP-based organic compounds such as 5CB (pentyl-cyanobiphenyl) are well known for their liquid crystal properties.[38] The synthesized ligands are soluble in chloroform, dichloromethane, acetone, tetrahydrofuran and insoluble in acetonitrile, water, diethylether, ethanol and methanol. The corresponding clusters, **CUB-Cn** (n =8, 12 and 16) and **CUB-CBP** have been synthesized by reacting CuI with the ligands in dichloromethane at room temperature. **CUB-C8** and **CUB-C12** have been obtained as viscous liquids whereas **CUB-C16** and **CUB-CBP** are solid powders. The clusters present the same solubility properties as the ligands. From UV-vis absorption analysis, the coordination of the ligand is revealed by a new absorption band around 300 nm (Figure S1). This band must originate from the charge-transfer transition namely X,MLCT.[39] For **CUB-CBP**, the latter is masked by the absorption band of the CBP moiety. The formula $[Cu_4I_4L_4]$ (L = ligand) is confirmed by elemental analysis, ^1H and ^{31}P NMR analyses.

The DSC traces and SAXS patterns of **CUB-Cn** (n = 8, 12 and 16) are reported in SI and all the data related to their mesomorphic properties are reported in Table 1. **CUB-C8** presents a single glass transition centered at T_g = 3.5 °C (Figure S2). From POM observations, the compound is in an isotropic soft viscous and malleable state at room temperature and is a brittle solid in an isotropic glassy state below T_g. SAXS pattern of the isotropic fluid phase at 20 °C displays three scattering signals centered at 34.3, 11.3 and 4.1 Å (Figure S3). These mean distances are attributed respectively to the distance between the **CUB-C8** functionalized clusters, the $[Cu_4I_4]$ inorganic cores and the C8 alkyl chains in a disordered state. Despite the sharper peak in the small angle region of the SAXS patterns, POM observations clearly indicate that this compound remains amorphous over the whole explored temperature range. Similarly, **CUB-C12** displays only a reversible glass transition centered at T_g = 15.5 °C, corresponding to the thermal transition between an isotropic glassy state and a viscous isotropic state as confirmed by POM observations. **CUB-C16** presents one first order reversible transition centered at $T_{cryst.}$ = 33 °C above which the compound is in an isotropic fluid state as revealed by POM observations. Below this transition, a weak birefringence appears and the compound becomes solid and brittle. This transition corresponds to the melting/crystallization of the compound (Figure S2). Compared with **CUB-C8** and **CUB-C12**, the increase of the chain length favours the crystallization and a melting point instead of a glass transition is observed. The SAXS pattern of **CUB-C16** recorded at 50 °C displays three similar scattering signals corresponding to the mean distances between the clusters at various scales in a poorly organized phase. The sharpening of the halo at around $2\theta = 20°$ (~ 4.1 Å) observed by lowering the temperature (pattern at -20 °C in Figure S3) agrees with the crystallisation of the long alkyl chains. In the small angle region, the appearance of a second order reflection at $2\theta = 3.8°$ indicates a short range organization of the compound. The limited number of reflections on the XRD pattern and the poor quality of the textures observed by POM does not allow more details on the molecular organization of **CUB-C16** in the crystalline phase.

Table 1. DSC and XRD data of **CUB-Cn** (n = 8, 12 and 16) and **CUB-CBP**.

Compound	Transition temperatures (°C) (ΔH in J.g^{-1}, ΔC_p in J.g^{-1}.K^{-1}) [a]	Diffraction peaks (Å)
CUB-C8	G 6.0 (ΔC_p = 0.12, T_g) I I 1.1 (ΔC_p = 0.93, T_g) G	34.3, 11.3, 4.1 (20 °C)
CUB-C12	G 17.0 (ΔC_p = 0.12, T_g) I I 13.8 (ΔC_p = 0.11, T_g) G	-
CUB-C16	Cr 41.0 (ΔH = 32.03) I I 24.6 (ΔH = -30.73) Cr	41.4, 11.2, 4.4 (50 °C)
CUB-CBP	G 25.2 (ΔC_p = 0.43, T_g) Sm_A 104.1 (ΔH = 8.19) I I 98.3 (ΔH = -8.13) Sm_A 22.4 (ΔC_p = 0.325, T_g) G	24.5, 11.3, 4.4 (120 °C) 58.7, 29.2, 11.9, 4.4 (80 °C)

[a] Sm_A = Smectic A phase, G = glassy state, Cr = crystalline phase; I = isotropic liquid. T in °C, ΔH in J.g^{-1} and ΔCp^* in J.g^{-1}.K^{-1} are given in parentheses.

CUB-Cn (n= 8, 12, 16) compounds are thus deprived of mesomorphic properties. This contrasts with Mn_{12} polyoxometallate compounds functionalized by similar gallate derivatives carrying three long alkyl chains, for which thermotropic cubic mesophases have been reported.[40] This can be explained by an insufficient coating of the long alkyl chains around the $[Cu_4I_4]$ cluster core in order to generate an isotropic spherical interface able to induce a proper molecular segregation into a 3D array. Heating at high temperatures to further increase the fluidity of the phases did not lead to inverse melting and no "re-entrance of the isotropic phase" was observed.[41] All **CUB-Cn** stay in an isotropic state up to 160 °C as confirmed by SAXS measurements.

As shown in Figure 2a, the DSC curves of **CUB-CBP** present a reversible second order glass transition around 20 °C (T_g) and a first order reversible thermal transition centered at 100 °C. The material is fluid and appears completely black under crossed polarizers above 100 °C. Upon cooling from the isotropic phase, a fluid and birefringent phase readily develops which correspond to the formation of a liquid crystalline phase. The texture observed presents large homeotropic domains and Maltese crosses, typical of a smectic A phase (Figure 2b).[42] Below the glass transition, the material is no more fluid and the persistent texture of the smectic A phase is hardly deformable. **CUB-CBP** was found to be stable up to 220 °C. Under UV irradiation at 350-400 nm, the compound appears to be highly emissive in the blue-green region (*vide supra* and Figure S4).

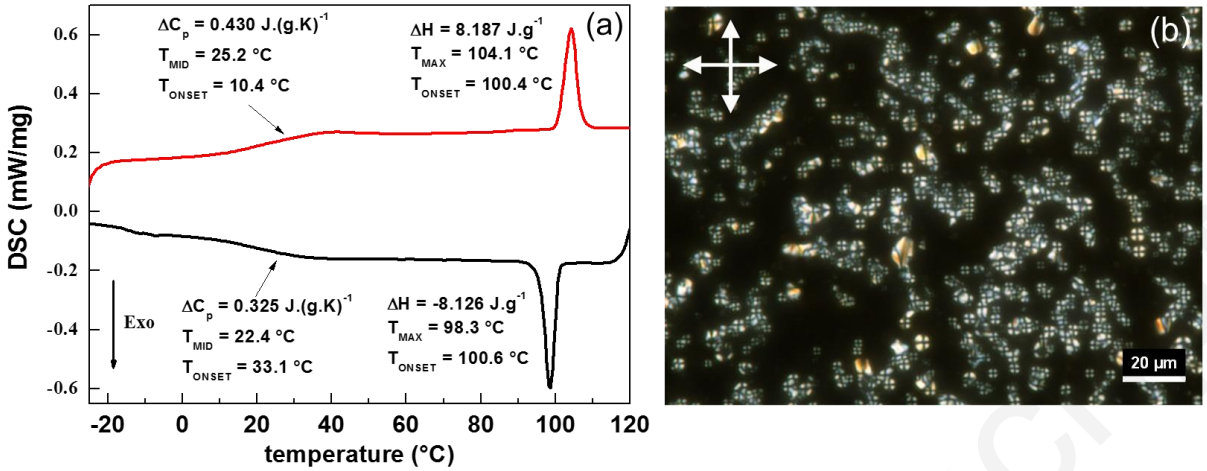

Figure 2. (a) DSC curves of **CUB-CBP** (red: second heating curve, black: first cooling curves, 10 °C/min). (b) Texture observed by optical microscopy between crossed-polarizers upon cooling (symbolized by the cross in the corner of the picture) at 95 °C revealing the co-existence of black homeotropic regions and Maltese crosses.

The SAXS patterns recorded at 120 °C is typical of a poorly organized isotropic phase and displays three broad low intensity halos centred at 24.5, 11.3 and 4.4 Å, corresponding respectively to the mean distances between the **CUB-CBP** clusters, the $[Cu_4I_4]$ inorganic cores and the C12 alkyl chains bearing the cyanobiphenyl groups (Figure 3). The patterns recorded at different temperatures between the glass transition and the clearing point (20-100 °C) are all similar and confirm the formation of a lamellar liquid crystalline phase. They present two equidistant sharp reflections at 58.7 and 29.2 Å (at 80 °C, corresponding to (001) and (002) reflections) with reciprocal spacing of 1:2 ratio, due to the lamellar order. The broad signal at 11.9 Å ($2\theta = 7.4°$), not commensurate with the two previous peaks, is attributed to some short range order of the $[Cu_4I_4]$ cores inside the lamellas. Another broad and diffuse halo is observed at 4.4 Å ($2\theta = 21°$) and corresponds to the lateral short-range order of the molten alkyl chains and the mesogenic CBP moieties. These data indicate an organization, in which the peripheral mesogenic groups carried by the phosphine ligands are equally distributed on either side of the $[Cu_4I_4]$ inorganic core in a compact manner. Such micro-segregated smectic structure is commonly observed with cyanobiphenyl end-capped molecules.[31,32,33,40] From the calculated volume of the functionalized molecular cluster,[43] the surface of each CBP moiety can be estimated to 32 $Å^2$. This value is large compare with the expected cross-sectional area of 22-24 $Å^2$ for a CBP group arranged normal to the smectic layers.[44] This implies that in the present smectic A arrangement, the CBP moieties are interdigitated and densely packed into organic sublayers. The interlayer periodicity *d* (58.7 Å) is slightly shorter than the length of the molecule in a fully extended configuration, estimated to be around 71 Å,[45] in accordance with a cylindrical molecular conformation organized into layers with an interdigitation of the CBP groups into organic sublayers. A possible model for such an organization is presented in Figure 4. In order to validate this liquid crystalline organization of the **CUB-CBP** mesogens, Molecular Dynamics (MD) simulations were carried out at 333 K. The calculations support the suggested model. After structure optimization, the layered structure with a segregation between the cubane clusters, the alkyl chains and the cyanobiphenyl fragments is preserved (Figure S5) and the majority of the cyanobiphenyl fragments remains confined and strongly interdigitated into nitrogen rich organic sublayers even if some of them are also expelled into the alkyl chains layers. Note that to account for the value of the cross-section of the cyanobiphenyl fragments and to produce a reasonable packing density in the alkyl chain sublayers, the polymethylene spacers should be conformationally disordered (molten state) and not all in an anti-conformation. The lamellar structure thus originates from the anisotropic arrangement of the ligands surrounding the $[Cu_4I_4]$ cluster cores, leading to the segregated organization into inorganic and

organic sublayers. As already stated, similar organisation has been already been proposed for other unconventional cores bearing cyanbiphenyl mesogenic groups.[31,32,33,Erreur ! Signet non défini.] At lower temperature, the compound is in solid state keeping the smectic A organization.

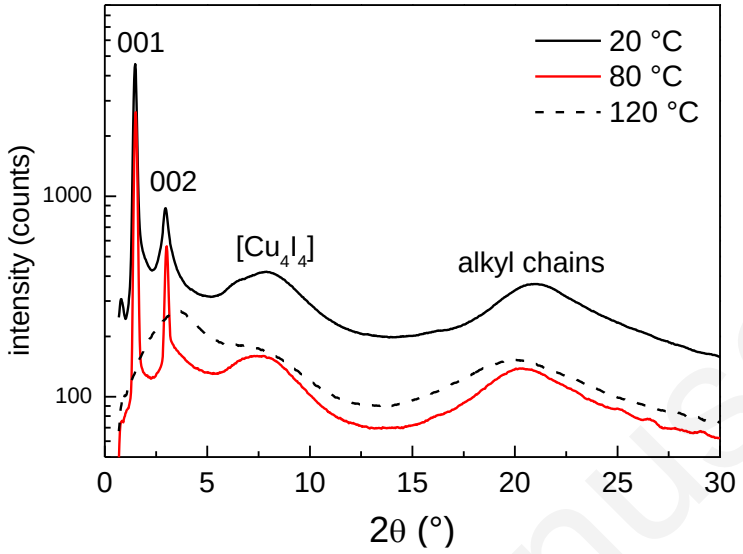

Figure 3. SAXS patterns of **CUB-CBP** collected at 120 °C (isotropic phase), at 80 °C (LC smectic A phase) and at 20 °C (solid smectic A phase).

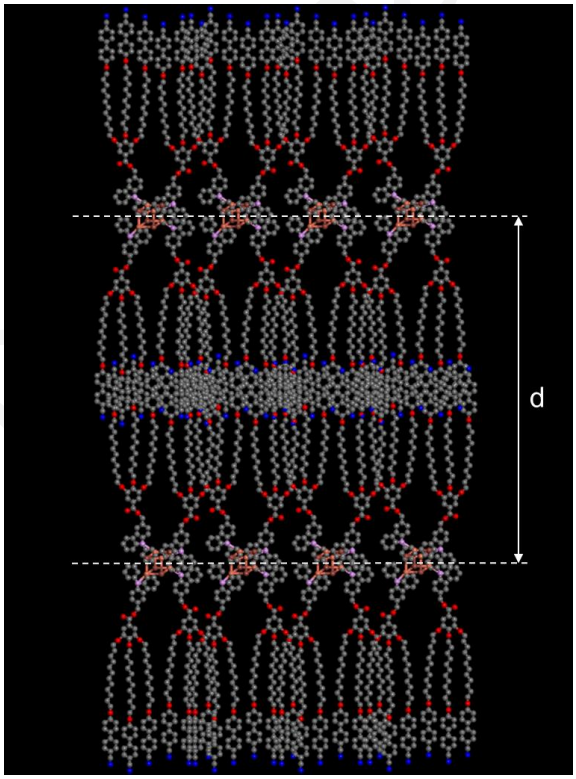

Figure 4. Model for the organization of the **CUB-CBP** clusters in the liquid crystalline smectic A phase presenting alternating inorganic and organic sublayers with d ~ 60 Å. Carbon atoms are in grey, oxygen in red, nitrogen in blue, phosphorus in purple and $[Cu_4I_4]$ cluster core in pink.

Optical properties.

Thermochromism. At room temperature, **CUB-C8** and **CUB-C12** are colorless sticky materials whereas **CUB-C16** and **CUB-CBP** are slightly yellowish solids under ambient light (all samples have been cooled from isotropic phases). **CUB-Cn** display a yellow emission under UV excitation, as shown in Figure 5. In contrast, **CUB-CBP** presents a blue emission in the same conditions. The compounds exhibit thermochromic luminescence properties. When they are cooled into liquid nitrogen at 77 K, their emission color become more intense and greener. When the samples are progressively warmed up to room temperature, the initial emissions are recovered, indicating a completely reversible thermochromism for all the clusters.

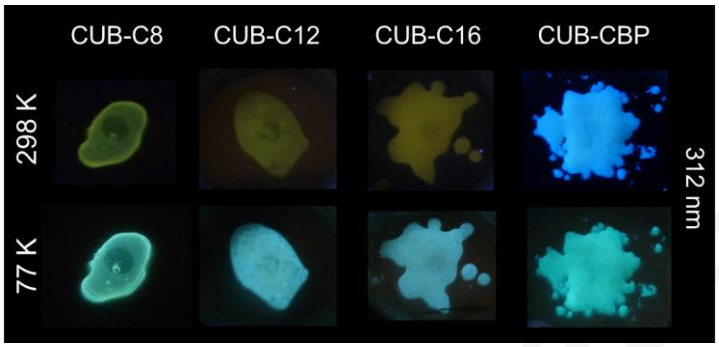

Figure 5. Photos of **CUB-Cn** (n = 8, 12, 16) and **CUB-CBP** under UV irradiation (lamp 312 nm) at 298 and 77 K.

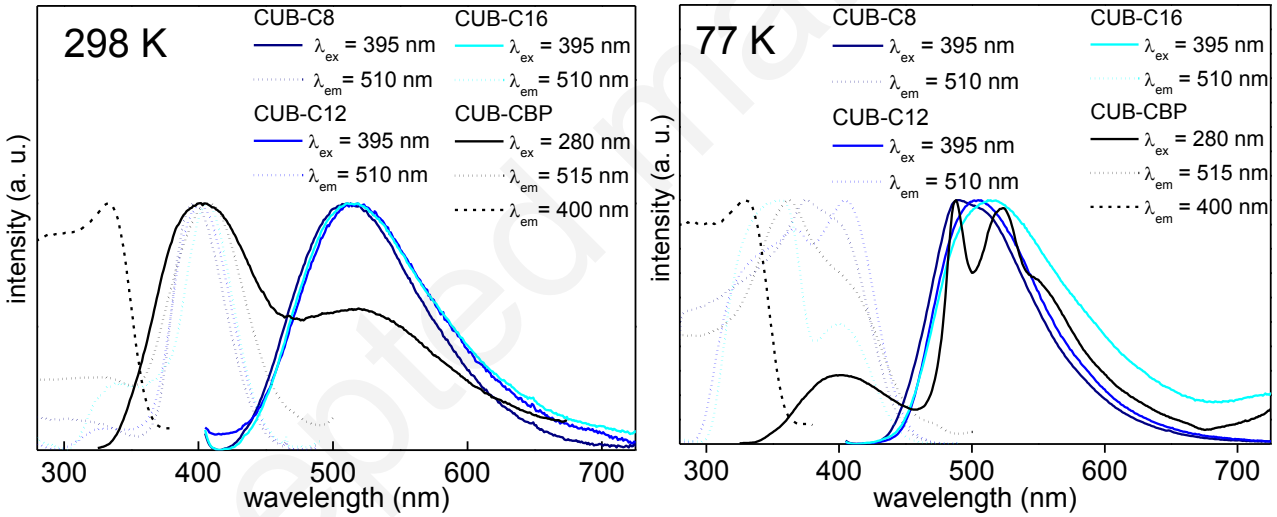

Figure 6. Solid-state luminescence spectra of **CUB-Cn** and **CUB-CBP** (after cooling from the isotropic phases), at 298 K and at 77 K, with emission spectra in plain lines and excitation spectra in dashed or dotted lines (normalized intensities).

Solid-state emission and excitation spectra recorded for all the clusters are shown in Figure 6 at room temperature and at 77 K. The corresponding data are reported in Table 2. At 298 K, for λ_{ex} = 395 nm, **CUB-Cn** (n = 8, 12, 16) present a similar unstructured broad emission band centered at λ_{max} = 512, 514 and 515 nm, respectively, in agreement with the green-yellow light observed. The corresponding absolute quantum yield values are Φ_{395} = <1, 3 and 2 %, respectively. This band is attributed to the classical LE band of copper iodide cubane clusters. Based on previous experimental and theoretical data,[39] this band is assigned to a $[Cu_4I_4]$ cluster centered excited state called ^{3}CC for 'Cluster Centered' and is essentially independent of the nature of the ligand. This triplet excited state is a combination of a halide-to-metal charge transfer (XMCT) and a copper-centered 3d → 4s, 4p transitions. At 77 K, the emission band of **CUB-Cn** are slightly blue shifted in accordance with the observed greener emission (Figure

6). Usually, $[Cu_4I_4]$ clusters bearing π-conjugated ligands exhibit luminescence thermochromism by the appearance at higher energy, upon cooling, of a new emission band (namely HE for High Energy) centered around 420 nm.[46] This blue band is, in contrast with the ^{3}CC one, 'ligand-centered' with a mixed charge-transfer (MLCT/XLCT) triplet excited state. The variation in temperature of the intensity of the LE and HE bands is at the origin of the luminescence thermochromism usually observed with the emissive state related to the LE band thermally populated from the HE one. This HE band is not observed for **CUB-Cn** compounds at 77 K but should appear at lower temperature.

CUB-CBP presents different luminescence properties by displaying at room temperature for λ_{ex} = 280 nm, two emission bands centered at λ_{max} = 404 and 519 nm (Figure 6). The first one is attributed to the CBP groups because the corresponding free ligand presents a similar emission band centered at λ_{max} = 378 nm (Figure S1) and the phosphine ligand without the CBP groups (ligand of **CUB-C12**) is not emissive in the same conditions. Moreover, CBP groups are reported to emit in the 400 nm range.[47] The second band observed at 519 nm is attributed to the LE cluster band (^{3}CC state), in agreement with the **CUB-Cn**. When the excitation wavelength decreases in energy, the intensity of this LE band relative to the CBP one increases and at λ_{ex} = 400 nm, only the LE band is observed (see following part in Figure 10). The quantum yield values related to the two emission bands are Φ_{280} = 9 % and Φ_{400} = 1 %. At 77 K, the relative intensities of the CBP-based and LE emission bands are inversed with a larger intensity for the LE band leading to the greener emission observed upon cooling down (Figure 5). The LE band also shows structured feature with the appearance of two new sharper bands at λ_{max} = 487 and 522 nm. These bands can be attributed to vibronic structure because of their similar excitation profiles (same energy level). **CUB-CBP** thus presents luminescence thermochromism with variation in temperature of the intensity of two emission bands. However, in opposite to 'classical' luminescence thermochromism of copper iodide clusters, the intensity of the LE band of **CUB-CBP** increases upon cooling down. In this case, the 'classical' HE band (MLCT/XLCT) is not observed and replaced by the CBP-based one but without thermal equilibrium between the two emissive states. This original behavior can be attributed to FRET (Förster Resonance Energy Transfer) mechanism with the CBP group acting as the donor and the cluster core as the acceptor.[48] This assumption is supported by the excitation profile corresponding to the LE band which overlaps the CBP emission band around 400 nm (Figure 6) and by the $[Cu_4I_4]$-CBP distance which can be estimated from the structural model to around 30 Å (simplified energy diagram in Figure S6). The transfer efficiency increases at lower temperature. ~~The detailed photophysical characterization of the FRET phenomenon is in progress and will be reported in due course.~~

Table 2. Photoluminescence data at 298 and 77 K of the clusters. CBP*g* corresponds to the ground sample.

CUB	T (K)	λ^{max}_{em} [λ_{ex}] (nm)
n = 8	298	512 [395]
	77	500 [395]
n = 12	298	514 [395]
	77	505 [395]
n = 16	298	515 [395]
	77	515 [395]
CBP	298	404, 519 [280] 519 [400]
	77	401, 487, 522 [280] 490, 522 [400]
CBP*g*	298	385, 549 [280] 536 [400]

	77	397, 494, 529 [280] 496, 529 [400]

Temperature dependent emission and influence of the molecular organization. In order to evaluate the influence of the molecular organization on the luminescence properties, the emission of **CUB-C16** and **CUB-CBP** has been recorded upon cooling from the isotropic state passing through temperature transitions. The spectra recorded from 60 to -10 °C for **CUB-C16** ($T_{cryst.}$ = 33 °C) are reported in Figure 7. Upon cooling, a significant intensity increase is observed along with a blue shift of the emission band. The variation in intensity can be explained by less efficient non-radiative phenomenon at lower temperature, usually observed by freezing a solution of clusters. This phenomenon along with the blue shift are directly related to the rigidochromism properties of the copper iodide clusters.[49] According to these properties, the effect is more pronounced nearby the crystallization temperature (Figure 7 insert).

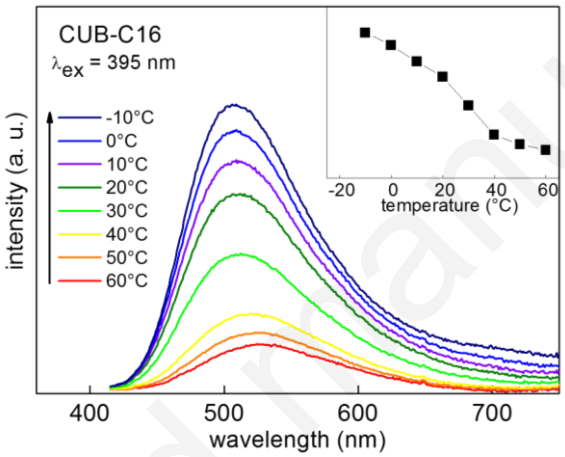

Figure 7. Temperature dependence of **CUB-C16** emission upon cooling from 60 down to -10 °C for λ_{ex} = 395 nm and in insert evolution in temperature of the intensity at λ_{max}.

The emission spectra of **CUB-CBP** recorded from 120 °C down to -150 °C are reported in Figure 8. Upon cooling, the intensity increases without marked changes of the shape of the two emission bands centered at 404 (CBP) and 519 (^{3}CC) nm. This can be explained by the decrease of non-radiative deactivation as already mentioned. However, the increase of the intensity is not linear with the temperature (Figure 8 insert). In the isoptropic phase (> 100 °C) the intensity is very weak and it rapidly increases when entering into the liquid crystalline smectic A phase around 100 °C. This can be correlated to the change of the rigidity between the isotropic phase and the LC phase which diminish the non-radiative phenomenon. It should also be noticed that the intensity increase upon further cooling inside the liquid crystalline phase is not linear and should also be correlated to drastic rigidity changes within the LC phase. Below the glass transition (< 25 °C), entering the solid state, the emission intensities still gradually increase but at a lower rate in agreement with lower rigidity modifications.

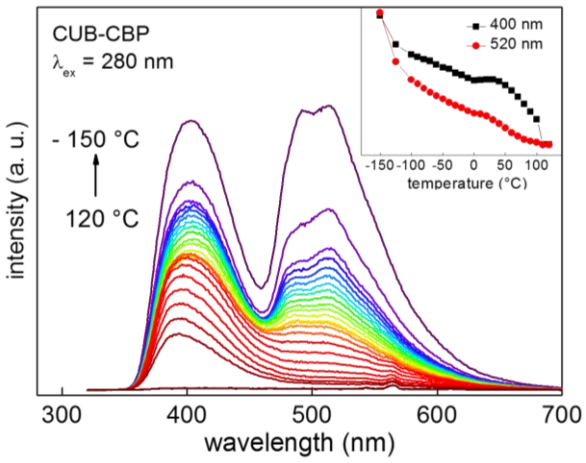

Figure 8. Temperature dependence of the **CUB-CBP** emission upon cooling from 120 down to -150 °C K, at λ_{ex} = 280 nm and in insert evolution in temperature of the intensity of the two bands at 400 (black squares) and 520 nm (red circles).

The temperature variation of the relative intensity of the LE and CBP bands also leads to change of the emission color. At high temperature, in the isotropic state (around 110°C), the sample exhibits a blue emission coming for the CBP band, the one of the CC band being almost absent. By lowering the temperature, the emission becomes greener as the intensity of the ^{3}CC band progressively increases exceeding at -150 °C that of the CBP band. The corresponding chromaticity coordinates in the CIE diagram (Commission Internationale de L'Eclairage 1931) are reported in Figure S7 and show marked color variation from deep blue to cyan. This relative change of the intensity of the two bands is not connected to a temperature effect but really correlated to the molecular organization. Indeed, **CUB-CBP** in solution displays a single blue emission band (λ_{max} = 363 nm) very similar to a spin-coated film (λ_{max} = 383 nm) at room temperature (Figure S8). These results indicates that the appearance of the ^{3}CC band is linked to a particular molecular order. In solution or in spin-coated film, there is no specific organization of the clusters just as in the isotropic phase. The ordering of the ligands leads to the ^{3}CC emission as observed in the LC state. This change of the CBP organization can be observed in the corresponding band position with a redshifted emission for aggregated state.[47] In our case, this redshift is observed between the isotropic state (λ_{max} = 394 nm) and the LC phase (λ_{max} = 404 nm). The emission of the solution and the spincoated film at higher energy agrees with less ordered phase with emission even reaching that of CBP monomers. Reorganization can be observed upon thermal treatment with the appearance of the CC band (Figure S8). Thus, the ^{3}CC band emission of the $[Cu_4I_4]$ cluster core is very sensitive to the molecular organization and in particular to the degree of aggregation of the CBP groups which seems to be optimal in the smectic phase. This dependence can be related to the FRET mechanism which probably occurs between this two emissive moieties. Indeed, FRET efficiency has been reported to be highly dependent to the donor-acceptor distance and to their respective orientation.[50]

Mechanochromism*. CUB-CBP** exhibits mechanochromic luminescence properties whereas **CUB-Cn** do not. Indeed, upon grinding or crushing, **CUB-CBP** exhibits a change of its emission color with the initial blue emission converted into a green-yellow one while its body color remains similar (Figure 9). The luminescence spectra of **CUB-CBP** before and after grinding (namely **CUB-CBP*g*)** at room temperature, are reported in Figure 10 (Table 2). The variation in intensity of the two bands in function of the excitation wavelength of **CUB-CBP*g is similar to the compound before grinding. From the spectra recorded at λ_{ex} = 280 nm, the grinding induces a significant red shift of the emission wavelength of the CC band while the CBP based one endorses a blue shift. For λ_{ex} = 400 nm, the shift of the ^{3}CC band (~25 nm) is obvious with the initial emission centered at λ_{max} = 517 nm shifting to 540 nm after the mechanical solicitation. **CUB-CBP*g*** also presents luminescence thermochromism by exhibiting a greener emission at low temperature (Figure 9). The emission spectra recorded at 77 K before and after grinding are

reported in Figure 10 for comparison. For λ_{ex} = 280 nm, the spectra are very similar with smaller blue and red shifts of the two CBP and ^{3}CC bands compared with those at 298 K. For λ_{ex} = 400 nm, the ^{3}CC bands are still structured with also a smaller red shift (6 nm). The effect of the grinding thus appears less pronounced at low temperature.

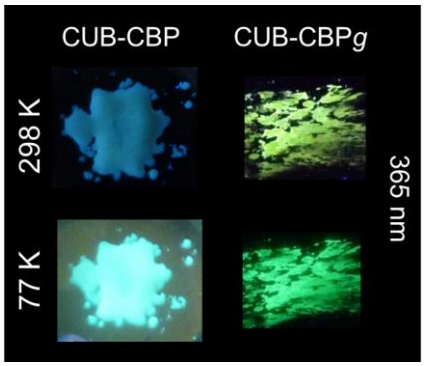

Figure 9. Photos under 365 nm (UV lamp) of **CUB-CBP** before and after grinding at 298 and 77 K.

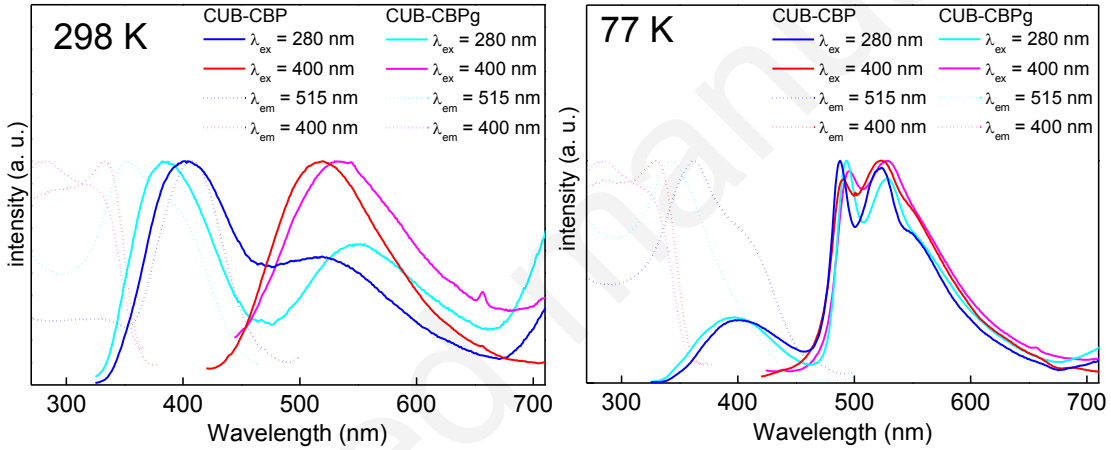

Figure 10. Solid-state luminescence spectra of **CUB-CBP** and **CUB-CBP*g*** at 298 K and at 77 K, with emission spectra in plain lines and excitation spectra in dotted lines (normalized intensities).

^{1}H liquid NMR spectra of the **CUB-CBP** before and after grinding are similar indicating that no chemical reaction related to adsorption or removal of atmospheric molecules was induced by the grinding. UV-vis. absorption (λ_{max} = 300 nm) and luminescence spectra in dichloromethane solution (λ_{max} = 360 nm for λ_{ex} = 280 nm) at room temperature, are also similar whether the cluster has been ground or not before dissolution, confirming that the molecular structure of the cluster is preserved after the mechanical solicitation. This is further supported by the comparable luminescence thermochromism exhibited by both compounds. **CUB-CBP** slowly recovers its initial phase and emission properties spontaneously at room temperature and this return can be accelerated upon thermal treatment (typically 100 °C, 30 min). When the sample is ground one more time, the shift of the emission is observed again which indicates reversibility of the phenomenon. SAXS analysis have been performed on **CUB-CBP*g*** at room temperature. As shown in Figure 11, the grinding process induces a broadening of the diffraction peak (001) compared with that of the initial compound. The narrow peak width is further recovered upon annealing at 100°C in accordance with the reversibility of the mechanochromism phenomenon. The peak broadening observed, indicates a transformation into a less ordered phase, sort of partial amorphization of the lamellar organization induced by the mechanical solicitation.

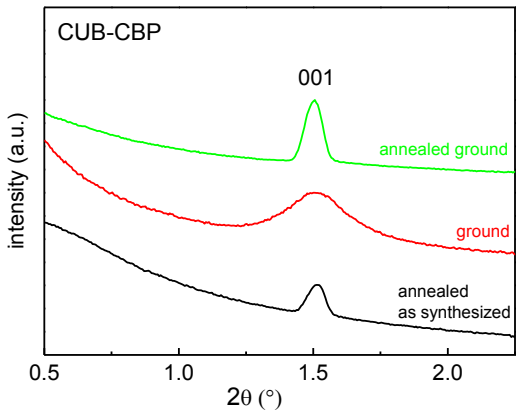

Figure 11. SAXS pattern recorded at 298 K of **CUB-CBP** before and after grinding and after annealing at 100 °C for 30 min.

A crystal-to-amorphous phase transformation is a common feature for mechanochromic compounds.[10] In particular, this is observed for the reported platinum liquid crystalline complex showing a disruption of the columnar mesophases with monomers emission leading to an isotropic phase with excimers emission.[21] This is different for the iridium complex for which a rigidochromism phenomenon is at the origin of the emission wavelength changes.[23] The local heating induced by the grinding process must play a role in the mechanochromic properties of **CUB-CBP**. The smectic solid → smectic CL transition occurs close to room temperature (T_g = 24 °C) meaning that a small increase in temperature can put the compound into the CL state. The gain of fluidity may help the system to reorganize into another less ordered metastable phase. This demonstrates the pertinence of liquid crystal properties to rationally synthesize mechanochromic compounds.

According to previous studies on mechanochromic copper iodide clusters,[27,28] the red shift of the LE emission observed upon grinding can be attributed to modification of the Cu-Cu interactions within the [Cu_4I_4] inorganic core. As previously mentioned, the LE band is cluster core centered in nature and its emission is correlated to the interatomic distances in the [Cu_4I_4] core. This LE emission indeed corresponds to a transition from a Cu-Cu nonbonding and Cu-I bonding HOMO to a strongly Cu-Cu bonding and Cu-I antibonding vacant orbital.[39] Therefore, the energy of the states mainly depends on the Cu-Cu bond distances with shorter distances leading to stabilization of the emissive state and a redshift of the emission. The mechanochromic properties of **CUB-CBP** can be thus explained by the shortening of the Cu-Cu bond distances upon grinding. This modification of the cluster molecular structure is connected to changes of intermolecular interactions upon disordering of the smectic A state. The blue shift observed for the CBP emission band is in agreement with modifications of the intermolecular order occurring through the ligands. Indeed, as already mentioned, the emission of CBP derivatives has been reported to be sensitive to their aggregation state (monomer *vs* dimer).[47] This agrees with alteration of the lamellar organization upon grinding and in particular of the organic sublayers. Note that the FRET efficiency seems to be unmodified in this case implying somehow preservation of the [Cu_4I_4]-CBP distance and their mutual orientation. The driving force of the mechanochromism phenomenon must be a 'constraint' molecular structure of **CUB-CBP** in the initial lamellar solid phase which relaxes upon grinding into a [Cu_4I_4] cluster core having stronger cuprophilic interactions. The formation of such Cu-Cu interactions is facilitated in the less ordered phase because of the increased molecular mobility. The constraints can be attributed to the anisotropic arrangement of the ligands around the cluster core. The lack of such specific organization can explain the absence of mechanochromic properties for the **CUB-Cn** compounds. This demonstrates the flexibility of the cluster core which adapts its geometry to the organization of the ligands.

Conclusion.

In order to rationally design and develop new stimuli-responsive materials with intriguing optical properties, the study of metallomesogens based on molecular copper iodide clusters has been conducted. Due to the unusual geometry of the inorganic $[Cu_4I_4]$ cubane core, only the functionalization with mesomorphic promoters, such as cyanobipenyl (CBP) groups, permit to successfully import liquid crystalline properties to the clusters. This particular compound, namely **CUB-CBP**, which brings together the photoactive CBP moieties and $[Cu_4I_4]$ cluster core, constitutes an original dual emissive system whose self-assembled supramolecular structures can be modified either by the temperature or mechanical stimuli resulting in luminescence properties changes. Indeed, **CUB-CBP** shows phase dependent emission properties and exhibits luminescent mechanochromic properties with reversible modification of the emission wavelength in response to mechanical solicitation. The grinding induces sort of crystalline-to-amorphous phase transition with a change of the self-assembled structures at the molecular level. The packing environment modification leads to cluster core geometry changes affecting the corresponding excited state. In opposite to most of the known systems for which mechanochromic properties are induced by a modulation of the intermolecular interactions between luminophores, here, they are due to the modulation of intramolecular interactions. In particular, the emission color change is attributed to the different strength of the cuprophilic interactions. The mechanochromism phenomenon clearly appears as a competition between inter and intramolecular interactions that can be easily modulated thanks to the mesomorphic properties. Detailed photophysical analyses of these newly synthesized cubane cluster containing soft materials will allow a deeper understanding of the inter-intramolecular interactions/structure relationship at the origin of the mechanochromism phenomenon. The anisotropy of the emission properties will be also evaluated. From this study, combining the rich photoluminescence properties of copper iodide clusters with the flexible self-assembly properties of liquid crystals appears to be very promising to develop original mechanochromic materials. Future studies aim at the synthesis of photoactive materials based on copper iodide liquid crystalline compounds presenting diverse structural geometries and molecular organizations.

Acknowledgments. The authors thank the CNRS and the Ecole Polytechnique for funding. Q. B. thanks the DGA for his Ph. D fellowship. D. Carrière (LIONS, CEA) and M. Impéror (Laboratoire de Physique des Solides, UMR CNRS 8502) are thanked for their help in SAXS measurements of the ground samples. Franck Camerel thanks GENCI for allocation of computing time under project c2016085032. We thank S. Bourcier (LCM, Ecole Polytechnique) for the mass spectrometry experiments.

Supporting Information Available. DSC curves of **CUB-Cn** compounds, SAXS patterns of **CUB-C8** and **CUB-C16**, microscope images of **CUB-CBP** under UV irradiation, chromaticity coordinates of **CUB-CBP** as a function of the temperature, UV-vis. absorption spectra of clusters and ligands, simplified energetic diagram of **CUB-CBP** and emission spectra of **CUB-CBP** in solution, spincoated before and after annealing or dropcasted are given in supplementary information. This information is available free of charge via the Internet at http://pubs.acs.org.

TOC Graphic

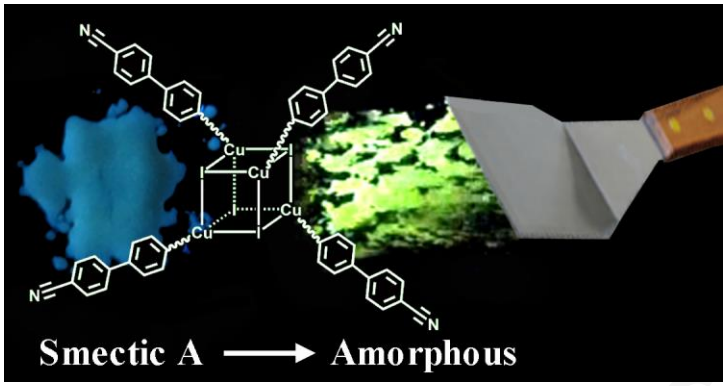

References.

(1) Kim, E.; Park, S. B. Chemistry as a Prism: A Review of Light-Emitting Materials Having Tunable Emission Wavelengths. *Chem. Asian J.* **2009**, *4* (11), 1646-1658.

(2) Hirata, S.; Watanabe, T. Reversible Thermoresponsive Recording of Fluorescent Images (TRF). *Adv. Mater.* **2006**, *18* (20), 2725-2729.

(3) Beyer, M. K.; Clausen-Schaumann, H. Mechanochemistry: The Mechanical Activation of Covalent Bonds. *Chem. Rev.* **2005**, *105* (8), 2921-2948.

(4) Wang, X.; Zhang, H.; Yu, R.; Dong, L.; Peng, D.; Zhang, A.; Zhang, Y.; Liu, H.; Pan, C.; Wang, Z. L. Dynamic Pressure Mapping of Personalized Handwriting by a Flexible Sensor Matrix Based on the Mechanoluminescence Process. *Adv. Mater.* **2015**, *27* (14), 2324-2331.

(5) Ariga, K.; Mori, T.; Hill, J. P. Mechanical Control of Nanomaterials and Nanosystems. *Adv. Mater.* **2012**, *24* (2), 158-176.

(6) Sagara, Y.; Kato, T. Mechanically Induced Luminescence Changes in Molecular Assemblies. *Nat. Chem.* **2009**, *1* (8), 605-610.

(7) Ciardelli, F.; Ruggeri, G.; Pucci, A. Dye-Containing Polymers: Methods for Preparation of Mechanochromic Materials. *Chem. Soc. Rev.* **2013**, *42* (3), 857-870.

(8) Sage, I.; Bourhill, G. Triboluminescent Materials for Structural Damage Monitoring. *J. Mater. Chem.* **2001**, *11* (2), 231-245.

(9) Balch, A. L. Dynamic Crystals: Visually Detected Mechanochemical Changes in the Luminescence of Gold and Other Transition-Metal Complexes. *Angew. Chemie Int. Ed.* **2009**, *48* (15), 2641-2644. and references therein.

(10) Weder, C. Mechanoresponsive Materials. *J. Mater. Chem.* **2011**, *21* (23), 8235-8236.

(11) Roberts, D. R. T.; Holder, S. J. Mechanochromic Systems for the Detection of Stress, Strain and Deformation in Polymeric Materials. *J. Mater. Chem.* **2011**, *21* (23), 8256-8268.

(12) Molin, M. D.; Verolet, Q.; Soleimanpour, S.; Matile, S. Mechanosensitive Membrane Probes. *Chem. - A Eur. J.* **2015**, *21* (16), 6012-6021.

(13) Chi, Z.; Zhang, X.; Xu, B.; Zhou, X.; Ma, C.; Zhang, Y.; Liu, S. J. Recent Advances in Organic Mechanofluorochromic Materials. *Chem. Soc. Rev.* **2012**, *41* (10), 3878-3896.

(14) Zhang, X.; Chi, Z.; Zhang, Y.; Liu, S.; Xu, J. Recent Advances in Mechanochromic Luminescent Metal Complexes. *J. Mater. Chem. C* **2013**, *1* (21), 3376-3390.

(15) Sagara, Y.; Yamane, S.; Mitani, M.; Weder, C.; Kato, T. Mechanoresponsive Luminescent Molecular Assemblies: An Emerging Class of Materials. *Adv. Mater.* **2016**, *28* (6), 1073–1095.

(16) Yamane, S.; Tanabe, K.; Sagara, Y.; Kato, T. Stimuli-Responsive Photoluminescent Liquid Crystals. *Top. Curr. Chem.* **2012**, *318*, 395–406.

(17) (a) Sagara, Y.; Kato, T. Brightly Tricolored Mechanochromic Luminescence from a Single-Luminophore Liquid Crystal: Reversible Writing and Erasing of Images. *Angew. Chemie* **2011**, *123* (39), 9294–9298. (b) Sagara, Y.; Yamane, S.; Mutai, T.; Araki, K.; Kato, T. A Stimuli-Responsive, Photoluminescent, Anthracene-Based Liquid Crystal: Emission Color Determined by Thermal and Mechanical Processes. *Adv. Funct. Mater.* **2009**, *19* (12), 1869–1875. and references therein. (c) Yamane, S.; Sagara, Y.; Mutai, T.; Araki, K.; Kato, T. Mechanochromic Luminescent Liquid Crystals Based on a Bianthryl Moiety. *J. Mater. Chem. C* **2013**, *1* (15), 2648-2656. (d) Mitani, M.; Yamane, S.; Yoshio, M.; Funahashi, M.; Kato, T. Mechanochromic Photoluminescent Liquid Crystals Containing 5,5′-Bis(2-Phenylethynyl)-2,2′-Bithiophene. *Mol. Cryst. Liq. Cryst.* **2014**, *594* (1), 1126121. (e) Mitani, M.; Ogata, S.; Yamane, S.; Yoshio, M.; Hasegawa, M.; Kato, T. Mechanoresponsive Liquid Crystals Exhibiting Reversible Luminescent Color Changes at Ambient Temperature. *J. Mater. Chem. C* **2016**, *4* (14), 275262760.

(18) S. Yagai, S. Okamura, Y. Nakano, M. Yamauchi, K. Kishikawa, T. Karatsu, A. Kitamura, A. Ueno, D. Kuzuhara, H. Yamada, T. Seki, H. Ito, Design Amphiphilic Dipolar π-systems for Stimuli-responsive Luminescent Materials using Metastable States. *Nat. Commun.*, **2014**, *5*, 4013-4023.

(19) Ren, Y.; Kan, W. H.; Henderson, M. A.; Bomben, P. G.; Berlinguette, C. P.; Thangadurai, V.; Baumgartner, T. External-Stimuli Responsive Photophysics and Liquid Crystal Properties of Self-Assembled "phosphole-Lipids." *J. Am. Chem. Soc.* **2011**, *133* (42), 17014-17026.

(20) Pucci, D.; Donnio, B. Handbook of Liquid Crystals 2nd edition, **2014**, *5*, 175-242.

(21) Kozhevnikov, V. N.; Donnio, B.; Bruce, D. W. Phosphorescent, Terdentate, Liquid-Crystalline Complexes of Platinum(II): Stimulus-Dependent Emission. *Angew. Chemie Int. Ed.* **2008**, *47* (33), 6286-6289.

(22) Krikorian, M.; Liu, S.; Swager, T. M. Columnar Liquid Crystallinity and Mechanochromism in Cationic platinum(II) Complexes. *J. Am. Chem. Soc.* **2014**, *136* (8), 2952-2955.

(23) Szerb, E. I.; Talarico, A. M.; Aiello, I.; Crispini, A.; Godbert, N.; Pucci, D.; Pugliese, T.; Ghedini, M. Red to Green Switch Driven by Order in an Ionic IrIII Liquid-Crystalline Complex. *Eur. J. Inorg. Chem.* **2010**, *2010* (21), 3270-3277.

(24) (a) Liu, Z.; Qiu, J.; Wei, F.; Wang, J.; Liu, X.; Helander, M. G.; Rodney, S.; Wang, Z.; Bian, Z.; Lu, Z.; Thompson, M. E.; Huang, C. Simple and High Efficiency Phosphorescence Organic Light-Emitting Diodes with Codeposited copper(I) Emitter. *Chem. Mater.* **2014**, *26* (7), 2368-2373. (b) Volz, D.; Zink, D. M.; Bocksrocker, T.; Friedrichs, J.; Nieger, M.; Baumann, T.; Lemmer, U.; Bräse, S. Molecular Construction Kit for Tuning Solubility, Stability and Luminescence Properties: Heteroleptic MePyrPHOS-Copper Iodide-Complexes and Their Application in Organic Light-Emitting Diodes. *Chem. Mater.* **2013**, *25* (17), 3414-3426. (c) Cariati, E.; Lucenti, E.; Botta, C.; Giovanella, U.; Marinotto, D.; Righetto, S. Cu(I) Hybrid Inorganic–organic Materials with Intriguing Stimuli Responsive and Optoelectronic Properties. *Coord. Chem. Rev.* **2016**, *306*, 566-614.

(25) Tsuge, K.; Chishina, Y.; Hashiguchi, H.; Sasaki, Y.; Kato, M.; Ishizaka, S.; Kitamura, N. Luminescent Copper(I) Complexes with Halogenido-Bridged Dimeric Core. *Coord. Chem. Rev.* **2016**, *306*, 636-651.

(26) Benito, Q.; Baptiste, B.; Polian, A.; Delbes, L.; Martinelli, L.; Gacoin, T.; Boilot, J. P.; Perruchas, S. Pressure Control of Cuprophilic Interactions in a Luminescent Mechanochromic Copper Cluster. *Inorg. Chem.* **2015**, *54* (20), 9821-9825.

(27) Perruchas, S.; Goff, X. Le; Maron, S.; Maurin, I.; Guillen, F.; Garcia, A.; Gacoin, T.; Boilot, J.-P. Mechanochromic and Thermochromic Luminescence of a Copper Iodide Cluster. *J. Am. Chem. Soc.* **2010**, *132* (32), 10967-10969.

(28) Benito, Q.; Goff, X. F. Le; Maron, S.; Fargues, A.; Garcia, A.; Martineau, C.; Taulelle, F.; Kahlal, S.; Gacoin, T.; Boilot, J.-P.; Perruchas, S. Polymorphic Copper Iodide Clusters: Insights into the Mechanochromic Luminescence Properties. *J. Am. Chem. Soc.* **2014**, *136*, 11311-11320.

(29) Wen, T.; Zhang, D.-X.; Liu, J.; Lin, R.; Zhang, J. A Multifunctional Helical Cu(I) Coordination Polymer with Mechanochromic, Sensing and Photocatalytic Properties. *Chem. Commun.* **2013**, *49* (50), 5660-5662.

(30) Shan, X.-C.; Jiang, F.-L.; Chen, L.; Wu, M.-Y.; Pan, J.; Wan, X.-Y.; Hong, M.-C. Using Cuprophilicity as a Multi-Responsive Chromophore Switching Color in Response to Temperature, Mechanical Force and Solvent Vapors. *J. Mater. Chem. C* **2013**, *1* (28), 4339-4349.

(31) (a) Campidelli, S.; Lenoble, J.; Barberá, J.; Paolucci, F.; Marcaccio, M.; Paolucci, D.; Deschenaux, R. Supramolecular Fullerene Materials: Dendritic Liquid-Crystalline Fulleropyrrolidines. *Macromolecules* **2005**, *38* (19), 7915–7925. (b) Dardel, B.; Guillon, D.; Heinrich, B.; Deschenaux, R. Fullerene-Containing Liquid-Crystalline dendrimers Basis of a Presentation given at Materials Discussion No. 4, 11–14 September 2001, Grasmere, UK. *J. Mater. Chem.* **2001**, *11* (11), 2814-2831.

(32) (a) Terazzi, E.; Suarez, S.; Torelli, S.; Nozary, H.; Imbert, D.; Mamula, O.; Rivera, J.-P.; Guillet, E.; Bénech, J.-M.; Bernardinelli, G.; Scopelliti, R.; Donnio, B.; Guillon, D.; Bünzli, J.-C. G.; Piguet, C. Introducing Bulky Functional Lanthanide Cores into Thermotropic Metallomesogens: A Bottom-Up Approach. *Adv. Funct. Mater.* **2006**, *16* (2), 157-168. (b) Cardinaels, T.; Driesen, K.; Parac-Vogt, T. N.; Heinrich, B.; Bourgogne, C.; Guillon, D.; Donnio, B.; Binnemans, K. Design of High Coordination Number Metallomesogens by Decoupling of the Complex-Forming and Mesogenic Groups: Nematic and Lamello-Columnar Mesophases. *Chem. Mater.* **2005**, *17*, 6589-6598. (c) Date, R. W.; Iglesias, E. F.; Rowe, K. E.; Elliott, J. M.; Bruce, D. W. Metallomesogens by Ligand Design. *Dalton Trans.* **2003**, 1914-1931. (d) Camerel, F.; Ziessel, R.; Donnio, B.; Guillon, D. Engineering of an Iron–terpyridine Complex with Supramolecular Gels and Mesomorphic Properties. *New J. Chem.* **2006**, *30* (2), 135-139.

(33) (a) Molard, Y.; Dorson, F.; Cîrcu, V.; Roisnel, T.; Artzner, F.; Cordier, S. Clustomesogens: Liquid Crystal Materials Containing Transition-Metal Clusters. *Angew. Chemie Int. Ed.* **2010**, *49* (19), 3351–3355. (b) Cîrcu, V.; Molard, Y.; Amela-Cortes, M.; Bentaleb, A.; Barois, P.; Dorcet, V.; Cordier, S. From Mesomorphic Phosphine Oxide to Clustomesogens Containing Molybdenum and Tungsten Octahedral Cluster Cores. *Angew. Chemie* **2015**, *127* (37), 11071–11075. (c) Nayak, S. K.; Amela-Cortes, M.; Neidhardt, M. M.; Beardsworth, S.; Kirres, J.; Mansueto, M.; Cordier, S.; Laschat, S.; Molard, Y. Phosphorescent Columnar Hybrid Materials Containing Polyionic Inorganic Nanoclusters. *Chem. Commun.* **2016**, *52* (15), 3127-3130. (d) Molard. Y. Clustomesogens: Liquid Crystalline Hybrid Nanomaterials Containing Functional Metal Nanoclusters. *Acc. Chem. Res.*, **2016**, *49*, 1514-1523.

(34) Leising, R. A.; Grzybowski, J. J.; Takeuchi, K. J. Synthesis and Characterization of Six-Coordinate Ruthenium(II) Complexes That Contain Trans Spanning Diphosphine Ligands. *Inorg. Chem.*, **1988**, *27*, 1020-1025.

(35) Camerel, F.; Ulrich, G.; Ziessel, R. New Platforms Integrating Ethynyl-Grafted Modules for Organogels and Mesomorphic Superstructures. *Org. Lett.*, **2004**, *6*, 4171-4174.

(36) Kouwer, P. H. J.; Pourzand, J.; Mehl, G. H. Disc-shaped Triphenylenes in a Smectic Organisation. *Chem. Commun.*, **2004**, 66-67.

(37) Benito, Q.; Fargues, A.; Garcia, A.; Maron, S.; Gacoin, T.; Boilot, J.-P.; Perruchas, S.; Camerel, F. Photoactive Hybrid Gelators Based on a Luminescent Inorganic $[Cu_4I_4]$ Cluster Core. *Chem. - A Eur. J.* **2013**, *19* (47), 15831-15835.

(38) (a) Chandrasekhar, S. Liquid Crystals. 2nd Edition. New York: Cambridge University Press, **1992.** (b) Chuard, T.; Deschenaux, R.; Hirsch, A.; Schönberger, H. A Liquid-Crystalline Hexa-Adduct of Fullerene. *Chem. Commun.* **1999**, *35* (20), 2103-2104. (c) Deschenaux, R.; Donnio, B.; Guillon, D. Liquid-Crystalline Fullerodendrimers. *New J. Chem.* **2007**, *31* (7), 1064-1073.

(39) Perruchas, S.; Tard, C.; Le Goff, X. F.; Fargues, A.; Garcia, A.; Kahlal, S.; Saillard, J.-Y.; Gacoin, T.; Boilot, J.-P. Thermochromic Luminescence of Copper Iodide Clusters: The Case of Phosphine Ligands. *Inorg. Chem.* **2011**, *50* (21), 10682-10692.

(40) Terazzi, E.; Bourgogne, C.; Welter, R.; Gallani, J.-L.; Guillon, D.; Rogez, G.; Donnio, B. Single-Molecule Magnets with Mesomorphic Lamellar Ordering. *Angew. Chemie* **2008**, *120* (3), 500-505.

(41) (a) Terzis, A. F.; Vanakaras, A. G.; Photinos, D. J. Conformational Phase Transitions and Re-Entrance Phenomena in Dendromesogens. *Mol. Cryst. Liq. Cryst.* **2000**, *352*, 265-274. (b) Crisanti, A.; Leuzzi, L. Stable Solution of the Simplest Spin Model for Inverse Freezing. *Phys. Rev. Lett.* **2005**, *95* (8), 087201.

(42) Dierking, I. *Textures of Liquid Crystals*, Wiley-VCH, Weinheim, **2003**.

(43) Volume of the cluster: $V_{cluster} = M/(\rho NA) = 11421$ Å^3 with M = 6877.82 g.mol^{-1} and $\rho = 1$ g.cm^{-3}.
Surface of the cluster: $AM = V_{cluster}/d = 195$ Å^2 with d = 58.7 Å.
Surface of the CBP moiety: $am = AM/6 = 32$ Å^2.

(44) Campidelli, S.; Vázquez, E.; Milic, D.; Prato, M.; Barberá, J.; Guldi, D. M.; Marcaccio, M.; Paolucci, D.; Paolucci, F.; Deschenaux, R. Liquid-Crystalline Fullerene–ferrocene Dyads. *J. Mater. Chem.* **2004**, *14* (8), 1266-1272.

(45) Estimated length using the Chem3D program.

(46) Tard, C.; Perruchas, S.; Maron, S.; Le Goff, X. F.; Guillen, F.; Garcia, A.; Vigneron, J.; Etcheberry, A.; Gacoin, T.; Boilot, J.-P. Thermochromic Luminescence of Sol−Gel Films Based on Copper Iodide Clusters. *Chem. Mater.* **2008**, *20* (22), 7010-7016.

(47) (a) Ikeda, T.; Kurihara, S.; Tazuke, S. Excimer formation kinetics in liquid-crystalline alkylcyanobiphenyls. *J. Phys. Chem.* **1990**, *94* (17), 6550-6555. (b) Piryatinskiĭ, Y. P.; Yaroshchuk, O. V. Photoluminescence of Pentyl-Cyanobiphenyl in Liquid-Crystal and Solid-Crystal States. *Opt. Spectrosc.* **2000**, *89* (6), 860-866. (c) Bezrodna, T.; Melnyk, V.; Vorobjev, V.; Puchkovska, G. Low-Temperature Photoluminescence of 5CB Liquid Crystal. *J. Lumin.* **2010**, *130* (7), 1134-1141.

(48) Broussard, J. A.; Rappaz, B.; Webb, D. J.; Brown, C. M. Fluorescence Resonance Energy Transfer Microscopy as Demonstrated by Measuring the Activation of the Serine/threonine Kinase Akt. *Nat. Protoc.* **2013**, *8* (2), 265-281.

(49) Roppolo, I.; Celasco, E.; Sangermano, M.; Garcia, A.; Gacoin, T.; Boilot, J.-P.; Perruchas, S. Luminescence Variation by Rigidity Control of Acrylic Composite Materials. *J. Mater. Chem. C* **2013**, *1* (36), 5725-5732.

(50) Valeur, B. *Molecular Fluorescence, Principles and Applications*, Wiley-VCH, **2009**.